Ultra-Low-Power PPG Analog Signal Processing Circuit for Continuous Blood Pressure Estimation

Ruben Ruiz-Mateos Serrano*, Dai Jiang† and Andreas Demosthenous†
Email:{rr632@cam.ac.uk, d.jiang@ucl.ac.uk, a.demosthenous@ucl.ac.uk}
*Department of Engineering (Division B), University of Cambridge, Cambridge, UK
†Department of Electronic and Electrical Engineering, University College London, London, UK

***Abstract*—This paper describes a novel photoplethysmography-based blood pressure estimation circuit developed as a non-invasive and continuous alternative to current clinical blood pressure monitoring devices. The system integrates the functionalities of analogue front-end and analogue-to-digital converter elements in conventional photoplethysmography sensors and extracts features related to blood pressure on chip. The topology operates in analogue domain, current mode and ultra-low-power, thus suppressing digitisation and current-to-voltage conversion errors and reducing overall power consumption. The circuit has been designed in CMOS 65 nm technology. It employs a 1.5 V supply, consumes ∼345 nW (five times less power than state-of-the-art) and generates feature voltages with a 50 mV max. deviation. A linear regressor trained with the extracted features achieves 0.7±0.9 mmHg accuracy (grade A performance). The operation of the topology is described and results depicting its performance are presented[1].**

***Index Terms*—BP, monitoring, non-invasive, PPG, sensor**

I. Introduction

Hypertension is a risk factor for potentially fatal cardiovascular, cerebrovascular and renal diseases. It affects 1.13 billion people in the world, a value that keeps rising due to the stressful lifestyle of modern society and worldwide sedentarism. The increases in blood pressure (BP) that lead to hypertension are gradual and accumulate over years before exhibiting symptoms; less than 20% of hypertensive patients are aware of their condition and have it under control. Regular monitoring of BP is thus essential to reduce the risk of undetected hypertension-triggered diseases [1].

Current BP measurements have two principal limitations for continual monitoring. Firstly, BP is generally measured on clinical settings, which is troublesome, increases infection risk and limits measurement frequency; secondly, BP measuring devices employ inflatable cuffs, which apply elevated pressure on the patient's arms or legs for intervals of time impractical for continuous monitoring [2].

Over the past decade, research has focused on developing cuff-less BP monitoring devices based on the analysis of changes in blood volume (BV), which is proportional to BP. Photoplethysmography (PPG) is an optical technique which measures the intensity of light reflected or transmitted through the skin, which varies with BV over time. PPG can be applied independently or jointly with electrocardiograms to determine arterial BV [3].

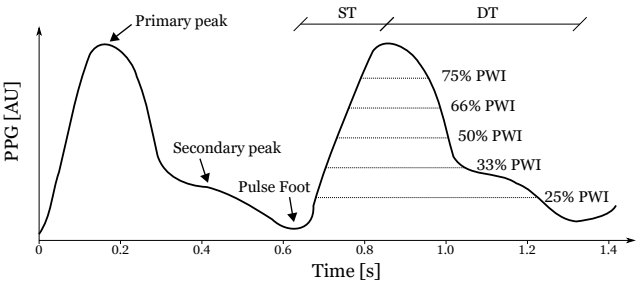

Fig. 1: PPG signal with BP time features extracted by PWA methods.

Methods for the estimation of BP from PPG can be classified into dual wave analysis (DWA), which calculate time interval characteristics of two physiological signals recorded simultaneously; and pulse wave analysis (PWA), which study time features extracted from PPG signals. PWA can be further distinguished into parametric or non-parametric. The former establish a fixed mathematical relationship between BP and features based on physiological models with patient-dependent coefficients. The latter avoid parameter calibration by employing machine learning to predict the relationship between BP and features. Typical PPG features which have been shown to relate to BP include the diastolic time (DT), systolic upstroke time (ST) and pulse width intervals (PWI) at various amplitude ratios of the primary peak (see Fig. 1) [4].

DWA offers accurate predictions because the relationship between physiological intervals and BP is well-understood, however, it requires two sensors which need to be synchronised and placed at specific locations. PWA only requires one sensor, however, it is more prone to motion artefacts and noise and the relationship between BP and features is unclear. Despite its limitations, PWA is potentially more appropriate for continuous BP monitoring. Particularly, non-parametric PWA offers the possibility of long-term, automatic calibration.

The optical readout module of PPG sensors generally consists of a light source, an optical receiver, an analogue front-end (AFE) which filters, amplifies and converts PPG current into voltage and an analogue-to-digital converter (ADC) which digitises the AFE output for further computer analysis. As Fig. 2 indicates, the largest source of power consumption and noise in current PPG sensors is the light source. Extensive

[1]This work was funded by the Engineering and Physical Research Council under grant EP/T001259/1

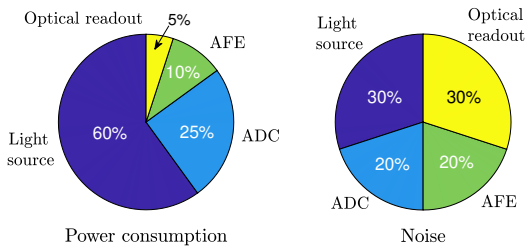

Light source [μW]	Optical readout [μW]	AFE [μW]	ADC [μW]	Reference
2	0.3	0.6	1.7	[5]
107	1.5	2	75	[6]
429	5.6	22.7	83	[7]
2400	120	380	2000	[8]
310	4.6	190	210	[9]

Fig. 2: Top: system level power and noise distribution in conventional PPG sensors. Bottom: power breakdown from literature values.

research into compressed sampling techniques has optimised its efficiency, however, a sampling limit has been reached which cannot be overcome. Similarly, research on optical receiver arrays has shown improved noise performance, however, it is limited by component efficiency. Optimisation efforts shift towards AFE and ADC. Light-to-digital conversion has been implemented to reduce most AFE noise, which arises from current-to-voltage conversion (CVC). Few efforts have considered the ADC, even though it is the second most power-hungry element and a large system noise contributor (20%). In fact, most proposed techniques often worsen ADC constraints with more complex quantisation methods. Removing the need for digitisation would improve system noise and power performance considerably.

This paper proposes a novel solution to PPG hardware limitations that integrates the AFE and ADC elements into a CMOS chip capable of continuous PPG feature extraction for BP estimation. The system operates in analog domain and current-mode, which avoids the power and noise produced by digitisation and CVC, and operates all transistors in weak-inversion, allowing for ultra-low-power consumption. In Section II, a system level description of the topology is presented. Section III shows simulation results demonstrating the performance of the circuit on real PPG data[2]. Section IV summarises the system architecture and results obtained.

II. System Description

As aforementioned, the relationship between PPG features and BP is ambiguous. Extensive number of algorithms have been proposed with a variable number of features [4], however, the correlation between each feature and BP varies across the literature and there is no consensus on whether increasing features benefits prediction. Considering this, the simple model in [11] has been imitated with five features: DT, ST and PWI at 25%, 50% and 75% of the primary peak (see Fig. 1).

A. Time-Domain Feature Extraction

As Fig. 3 shows, the feature extraction process follows two pipelines. PWI are obtained by calculating the magnitude of

[2]PPG signals were obtained from the MIMIC-III clinical database [10]

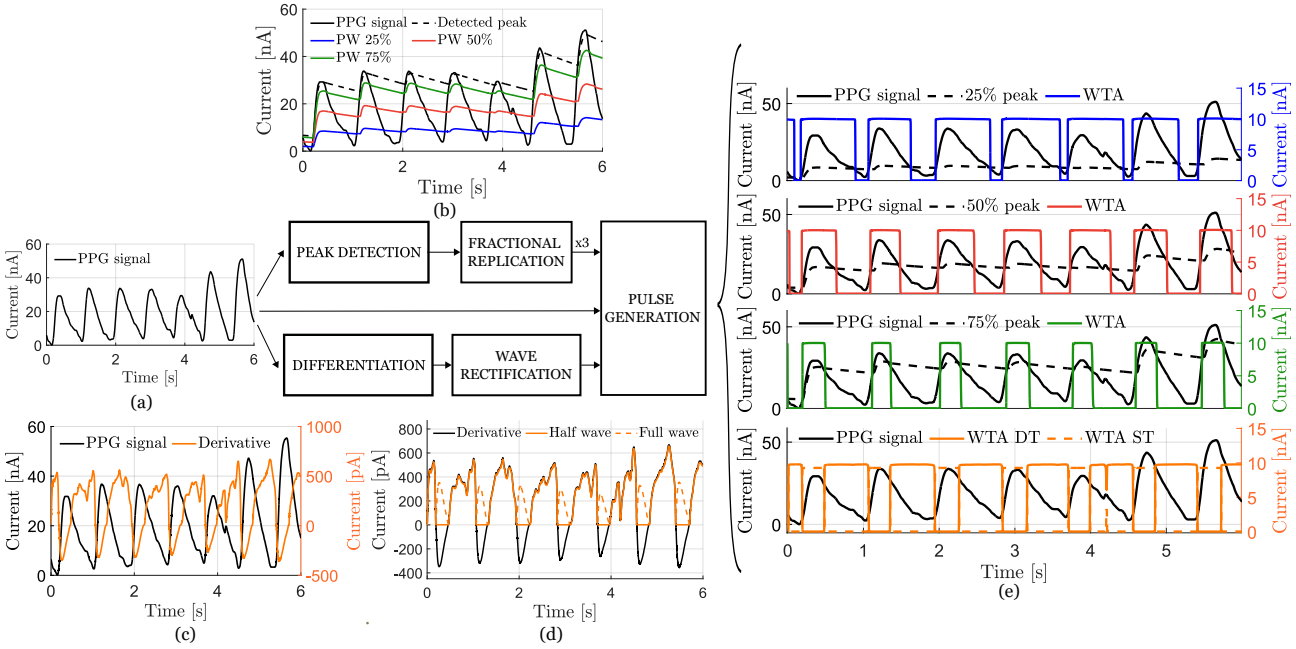

Fig. 3: System overview of proposed topology. PPG current from optical receiver (a) is processed in two pipelines: at the top, it is passed through a PD and CM to generate fractional duplicates of the peak of the PPG at 25%, 50% and 75% ratios (b); at the bottom, it is differentiated (c) and rectified (d). Both pipelines converge into WTA which generate pulses (e) whose width encodes the features of interest.

the primary peak and replicating it with reduction factors of 25%, 50% and 75% with current mirrors (CM). The input PPG is thresholded against these signals to define three square pulses (SP). ST and DT are extracted by taking the derivative of the input PPG, which encodes peaks and troughs at zero crossings. The derivative is half-wave rectified and thresholded against zero to define two reciprocal SP. The width of all pulses encodes the features of interest over time.

Peak detection is achieved with the peak detector (PD) in Fig. 4a. When I_{in} increases, the source voltage of M2 decreases, lowering the drain current of M3. Consequently, I_a discharges C_{par}, which decreases the gate voltage of M4 and opens it. M4 opening decreases the gate voltage of M3, hence restoring its drain current. I_{out} exactly replicates I_{in}. When I_{in} decreases, the opposite process occurs leading to the closing of M4, which ensures I_{out} holds its value. Charging and holding phase speeds are inversely proportional to the capacitances C_a and C_r and directly proportional to currents I_a and I_r, respectively.

The derivative of the input PPG is performed by the differentiator in Fig. 4b. The circuit consists of an input active load defined by diode-connected transistors M10 and M11, which is capacitively coupled to a bi-directional CM formed by M12-M15. The active load establishes low input impedance, ensuring a small time constant in the resulting RC topology, which yields a differentiation. Half-wave rectification is computed by the circuit in Fig. 4c. It consists of a source-connected PMOS NMOS pair and two CM. When $I_{in} > 0$, current flows in, turning all transistors on except M19. Both outputs replicate the input. When $I_{in} < 0$, current flows out, causing M19 to turn on and M18 and M20 to turn off. M18 yields zero current whereas M22 copies the inverted I_{in}.

SP generation is achieved with the winner-take-all circuit (WTA) in Fig. 4d. This circuit implements a competitive mechanism which reports the cell with the strongest input whilst suppressing all others. Transistors M6-M7 and M8-M9 perform local positive feedback loops which force their respective outputs I_{out1} and I_{out2} to saturate to I_b whenever the input of each cell becomes greater than the rest. KCL at the source of M7-M8 ensures all other outputs become zero. In the proposed circuit, all features require a WTA. For PWI, one of the input currents is the PPG signal and the other is the respective peak proportion; only the output of the cell containing the PPG signal input is employed. For DT and ST, the first input current is the half-wave rectified derivative of the PPG signal and the second is zero; a single WTA is required since the reciprocal outputs of the circuit automatically yield DT and ST features. WTA inputs must be strictly positive, thus explaining the need for half-wave rectification in the DT and ST extraction pipeline.

B. Time-to-Amplitude Domain Conversion

Once pulses are generated, the encoded information in time is translated into amplitude so it can be employed by a BP estimator. Since pulse magnitude remains constant, passive linear transformation of features from time to voltage can be performed with capacitors. From the definition of capacitance,

$$V(t) = \int_{t_0}^{t_f} \frac{I(t)}{C}\, dt \tag{1}$$

Assuming I is time-independent for the duration of each pulse (i.e. from t_0 to t_f), V is linearly related to I with a slope given by C. Equation (1) reveals a trade-off between output voltage resolution and magnitude range which needs to be optimised independently for each feature.

III. Results

Fig. 3 depicts nominal transient simulation results from the processing steps described in Section II. The PD successfully retains the maximum current of the input PPG and fractions it at the ratios of interest. The attack time captures the increases in current, however, peak underestimation can be observed, especially at larger amplitude cycles. The decay time of the PD optimises the trade-off between information loss and peak variation sensitivity. The encoded features are vulnerable to large cycle amplitude differences since at each rising edge the circuit encodes the peak of the previous cycle, however, drastic amplitude changes in BP are unusual.

The differentiator yields zero crossings at PPG peak and trough locations with few milliseconds delay. The pico-amp level signal is due to the charging time of capacitor C_{diff}, which needs to be large to capture slow changes. Simulation reveals accurate rectification with virtually zero offset.

The WTA successfully generate pulses whenever the PPG input becomes greater than the given peak ratio. DT and ST pulses encode peak and trough distances, however, the pulse saturation values are not clearly defined due to the low current values of the differentiator. A delay of few milliseconds can be observed at pulse rising and falling edges corresponding to local feedback saturation time.

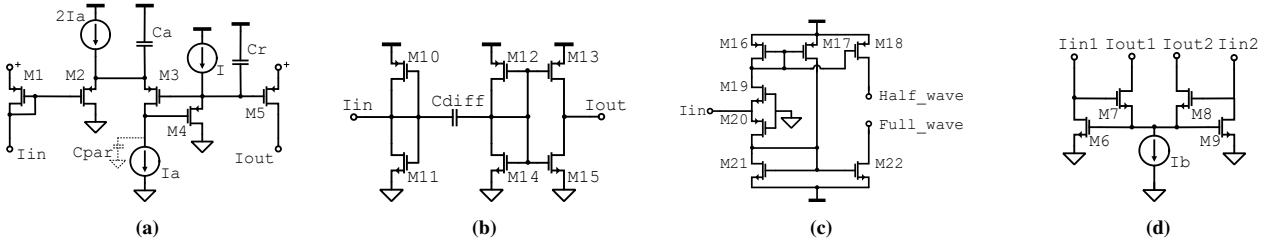

Fig. 4: Schematic diagrams of topologies employed by the proposed system. (a) Peak detector [12], (b) Current differentiator [13], (c) Full and half wave rectifier [14] and (d) Winner take all [15].

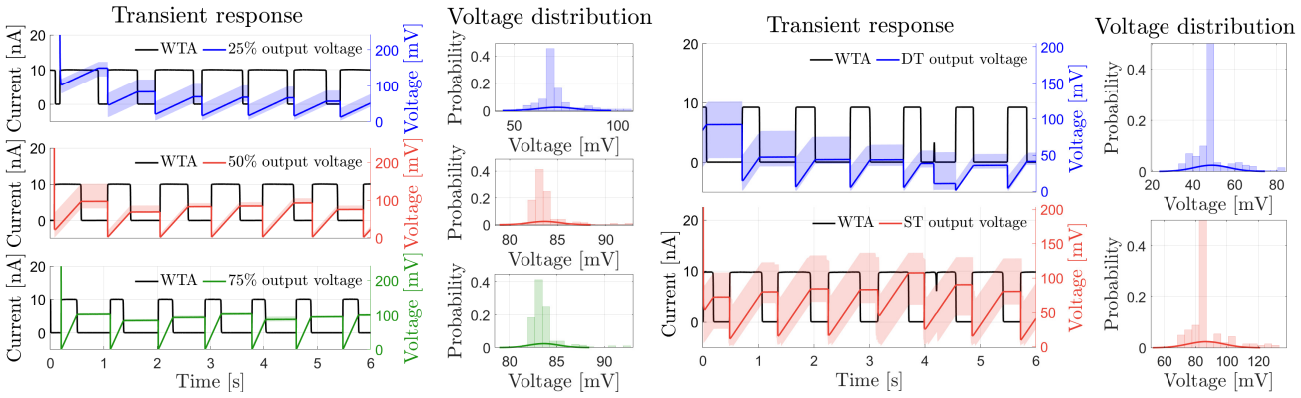

Fig. 5: Transient output of feature extraction system along with amplitude deviations of the constant voltage value obtained from the third pulse for (a) 25%, 50% and 75% PWI of the PPG peak and (b) ST and DT.

Fig. 5 shows the final output of the proposed system after time-to-voltage conversion. The output voltage increases linearly at a constant rate during a pulse and remains fixed when the input current is zero, with a value proportional to the width of the previous pulse. Transients due to initial capacitor discharge can be observed in all plots. Features with wider pulses generate a constant offset of few mV which is due to insufficient capacitor discharge time. Variations from component mismatch and manufacturing process errors reveal a maximum feature variation of ∼50mV. The mean variance decreases as the ratio of the PPG peak increases and is significantly greater for DT and ST features, indicating amplitude variability is dependent on pulse width and arises from fluctuations in saturation current.

The circuit has been designed in CMOS 65 nm technology, it requires a 1.5 V supply and consumes ∼345 nW of total power. A linear regressor was trained with the extracted features and achieved 0.7±0.9 mmHg accuracy, complying with grade A performance for cuff-less BP devices.

IV. Conclusion

In this paper a novel PPG-based BP feature extraction circuit has been presented as a non-invasive and continuous alternative to current clinical BP monitoring devices. The topology integrates AFE and ADC elements in conventional PPG sensors and extracts five PPG time features related to BP: PWI at 25%, 50% and 75% of the primary peak, DT and ST. The first three are calculated with fractional duplicates of PPG signal peaks. The latter two are obtained from the half-wave rectification of the derivative of PPG signals. The outputs from both pipelines are encoded in time domain with SP generated by WTA and converted to amplitude with capacitors. The circuit operates in analog domain, current-mode and weak-inversion, hence suppressing digitisation and CVC errors and reducing overall power consumption. Results describing the nominal response of the system have been presented, along with simulations indicating the effect of component mismatch and manufacture errors.

References

[1] P. M. Kearney, M. Whelton, K. Reynolds, P. K. Whelton, and J. He, "Worldwide prevalence of hypertension: a systematic review," *Journal of hypertension*, vol. 11, no. 9, 2004.

[2] G. Ogedegbe, "Barriers to optimal hypertension control," *The Journal of Clinical Hypertension*, vol. 10, no. 8, 2008.

[3] J. Solà and R. Delgado-Gonzalo, *The handbook of cuffless blood pressure monitoring*. Springer International Publishing, 2019.

[4] C. El-Hajj and P. A. Kyriacou, "A review of machine learning techniques in photoplethysmography for the non-invasive cuff-less measurement of blood pressure," *Biomedical Signal Processing and Control*, vol. 58, no. 1, 2020.

[5] A. Caizzone, A. Boukhayma, and C. Enz, "A 2.6 µW monolithic CMOS photoplethysmographic (PPG) sensor operating with 2 µW LED power for continuous health monitoring," *IEEE Transactions on Biomedical Circuits and Systems*, vol. 13, no. 6, 2019.

[6] Q. Lin, J. Xu, S. Song, A. Breeschoten, M. Konijnenburg, C. Van Hoof, F. Tavernier, and N. Van Helleputte, "A 119dB dynamic range charge counting light-to-digital converter for wearable PPG/NIRS monitoring applications," *IEEE Transactions on Biomedical Circuits and Systems*, vol. 14, no. 4, 2020.

[7] A. Sharma, A. Polley, S. B. Lee, S. Narayanan, W. Li, T. Sculley, and S. Ramaswamy, "A Sub-60-μA multimodal smart biosensing SoC with >80-dB SNR, 35-μA photoplethysmography signal chain," *IEEE Journal of Solid-State Circuits*, vol. 52, no. 7, 2017.

[8] M. Tavakoli, L. Turicchia, and R. Sarpeshkar, "An ultra-low-power pulse oximeter implemented with an energy-efficient transimpedance amplifier," *IEEE Transactions on Biomedical Circuits and Systems*, vol. 4, no. 1, 2010.

[9] K. N. Glaros and E. M. Drakakis, "A Sub-mW fully-integrated pulse oximeter front-end," *IEEE Transactions on Biomedical Circuits and Systems*, vol. 7, no. 3, 2013.

[10] A. Johnson, T. Pollard, and R. Mark, "MIMIC-III clinical database (version 1.4)," 2016.

[11] X. F. Teng and Y. T. Zhang, "Continuous and noninvasive estimation of arterial blood pressure using a photoplethysmographic approach," *Annual International Conference of the IEEE Engineering in Medicine and Biology - Proceedings*, vol. 4, no. 1, 2003.

[12] S. M. Zhak, M. W. Baker, and R. Sarpeshkar, "A low-power wide dynamic range envelope detector," *IEEE Journal of Solid-State Circuits*, vol. 38, no. 10, 2003.

[13] E. I. El-Masry and J. W. Gates, "Novel continuous-time current-mode differentiator and its applications," *IEEE Transactions on Circuits and Systems II: Analog and Digital Signal Processing*, vol. 43, no. 1, 1996.

[14] M. Yildirim, "Design of low-voltage and low-power current-mode DTMOS transistor based full-wave/half-wave rectifier," *Analog Integrated Circuits and Signal Processing*, vol. 106, no. 1, 2021.

[15] J. Lazzaro, S. Ryckebusch, M. A. Mahowald, and C. A. Mead, "Winner-take-all networks of O(N) complexity," in *Advances in Neural Information Processing Systems*, vol. 1, 1988.